

Oscillations in the dark energy equation of state: new MCMC lessons

Ruth Lazkoz, Vincenzo Salzano, Irene Sendra

*Fisika Teorikoaren eta Zientziaren Historia Saila, Zientzia eta Teknologia Fakultatea,
Euskal Herriko Unibertsitatea, 644 Posta Kutxatila, 48080 Bilbao, Spain*

24 October 2018

ABSTRACT

We study the possibility of detecting oscillating patterns in the equation of state (EoS) of the dark energy using different cosmological datasets. We follow a phenomenological approach and study three different oscillating models for the EoS, one of them periodic and the other two damped (proposed here for the first time). All the models are characterised by the amplitude value, the centre and the frequency of oscillations. In contrast to previous works in the literature, we do not fix the value of the frequency to a fiducial value related to the time extension of chosen datasets, but consider a discrete set of values, so to avoid arbitrariness and try and detect any possible time period in the EoS. We test the models using a recent collection of SNeIa, direct Hubble data and Gamma Ray Bursts data. Main results are: I. even if constraints on the amplitude are not too strong, we detect a trend of it versus the frequency, i.e. decreasing (and even negatives) amplitudes for higher frequencies; II. the centre of oscillation (which corresponds to the present value of the EoS parameter) is very well constrained, phantom behaviour is excluded at 1σ level and trend which is in agreement with the one for the amplitude appears; III. the frequency is hard to constrain, showing similar statistical validity for all the values of the discrete set chosen, but the best fit of all the scenarios considered is associated with a period which is in the redshift range depicted by our cosmological data. The “best” oscillating models are compared with Λ CDM using dimensionally consistent a Bayesian approach based information criterion and the conclusion reached is the non existence of significant evidence against dark energy oscillations.

1 INTRODUCTION

We have nowadays a great amount of independent data sets available for studying the present dynamical state of the Universe. High quality data coming from the Hubble diagram of Type Ia Supernovae (Riess et al. (2004); Astier et al. (2006); Clocchiati et al. (2006)); the measurements of cluster properties as the mass, the correlation function and the evolution with redshift of their abundance (Eke et al. (1998); Viana et al. (2002); Bahcall et al. (2003); Bahcall & Bode (2003)); the optical surveys of large scale structure (Pope et al. (2005); Cole et al. (2005); Eisenstein et al. (2005)); the anisotropies of the cosmic microwave background (de Bernardis et al. (2000); Spergel et al. (2003)); the cosmic shear measured from weak lensing surveys (van Waerbeke et al. (2001); Refregier (2003)) and the Lyman- α forest absorption (Croft et al. (1999); McDonald et al. (2005)) are evidences toward an *apparently clear* picture of our universe at present. It is characterised by: I. spatial flatness, II. a subcritical matter content, III. and accelerated expansion.

But the *clearness* of this sketch poses a more interesting and deeper problem: how can we interpret all these features

in the framework of a self-consistent theoretical cosmological model? This is the main task of modern cosmology and no unique answers have been given so far.

The Λ CDM model is the simplest (from a statistical point of view) and the most accepted (it is called *concordance model* just for this reason), and in this scenario acceleration is driven by the famous cosmological constant, Λ , which contributes to the energy/matter content of the Universe by more than a 74%. At the same time it requires the presence of a large amount of *cold dark matter* (about the 22% of total energy/matter content), i.e. non-baryonic matter which does not interact with electromagnetic radiation, but it is detectable only by its gravitational interaction with ordinary baryonic matter (which makes the remaining 4%). This model provides a good fit to most of the data (Tegmark et al. (2004); Seljak et al. (2005); Sánchez et al. (2006)) giving a reliable snapshot of the current Universe; but it is also affected by serious theoretical shortcomings that have motivated the search for alternative candidates generically referred to as *dark energy* or *quintessence*. Such models range from conventional scalar fields rolling down self-interaction potentials, to non-canonical scalar field models (phantom, k-essence, etc.); from phenomenological unified

models of dark energy and dark matter to alternative gravity theories (Peebles & Rathra (2003); Padmanabhan (2003); Copeland, Sami, and Tsujikawa (2006)).

Unfortunately, so many data are not yet able to give us a definitive answer about the origin and nature of the acceleration of the Universe; not able to solve the *coincidence problem*, (namely, why we are currently detecting an energy-density for dark energy which is quite equal to the one of dust matter); and not able to state what the right EoS of dark energy is.

Regarding the EoS, using current data one will be typically only able to infer that the dark energy effective EoS parameter w^1 is close to -1 . But any small deviation from this value could give a different theoretical scenario: if it is *exactly equal* (when of course referring to observational errors) to -1 , we have a cosmological constant; if it is larger than -1 , we have a quintessence model; while if it is smaller than -1 we have the so called phantom dark energy. In addition, the data seem to indicate that the fractional energy densities of two main components of the Universe, i.e. dark matter and dark energy, are very similar at present, and the label “coincidence problem” has been coined to refer to this striking similarity.

One of the most interesting solutions proposed to try and throw some light on these questions is *oscillating dark energy* (Dodelson (2000); Feng (2006); Sahni (2000)). Such a model can easily solve the coincidence problem in a very natural way due to periods of acceleration, and can be also used as a good candidate for the unification of the late time acceleration (the one observed at present) with inflation (an early time acceleration period). In this context we have to underline the difference between assessing a periodic or non-monotonic potential and an oscillating dark energy EoS. In many cases such potentials do not give rise to a periodic w ; one example can be found in Frieman (1995), where the proposed field is clearly periodic but the derived w can be well described by the CPL parametrization for dark energy introduced in Chevallier (2001) and Linder (2003).

In this paper we are going to follow the method from Linder (2006), by examining some directly proposed phenomenological periodic equations of state for the dark energy using different cosmological observations. Specifically, we are going to set constraints on the location of the centre of the range about which w oscillates and the amplitude of the oscillations, and we will also constrain the fractional energy density of matter.

Actually, in the models to be considered there is another important parameter, the frequency of the oscillation. Relevant though it is, leaving this parameter completely free leads to a high dimensionality statistical problem, but given the precision of the data available at present it seems that problems of that sort cannot be tackled satisfactorily; i.e. there seems to be not enough quality in the data to constrain more than two dark energy parameters Linder (2005); Sullivan (2008). In the literature on oscillating dark energy, the usual practice has been choosing a specific single value of this oscillation frequency and stick with it. In order to fix it one may resort to an argument by Linder (2006) which

suggests the lowest bound on this frequency for the data in use to be able to discriminate an oscillating behaviour from a monotonic one. We wish to carry out here a more thorough study of oscillating dark energy than previous works, and to this end we choose a discrete set of values of the frequency (above and below that bound) and then obtain constraints on the rest of parameters. Relaxing assumptions on the frequency, as compared to previous works, will allow us able to draw stronger conclusions; yet this is not the only novelty of our analysis, as will be shown in what follows.

In this exploration of possible oscillating patterns in the expansion of the Universe induced by the dark energy component we also find it interesting to consider non-periodic oscillating models. Specifically we deal with scenarios which display a similar start off to the popular oscillating model by Linder, but then depart from it as their amplitude gets smaller as z grows and the distance between nodes tends to converge to a specific value. In this direction, we propose a pair of models in which dark energy oscillations are modelled via special functions. Comparison between models of that sort and the usual trigonometric parametrization provides hints about which features in the oscillations are favoured or disfavoured.

Moreover, the present paper innovates in another direction: we choose a combination of datasets with interesting characteristics: we combine the statistically most powerful dataset available, the luminosity measurements of SNeIa, with other datasets: the luminosity measurements of Gamma Ray Bursts (GRBs) and direct Hubble data. GRBs are particularly useful for the study of oscillating models, as they typically inform us of higher redshifts than supernovae data, they improve the capability for detecting oscillating features (if they exist) at lower frequencies. In addition, the inclusion of the direct Hubble data can in principle enhance the sensitivity of our tests to the presence of oscillations, as the use of these data does not involve performing an averaging of the inverse of the Hubble factor, and then a possible smoothing of the oscillations is partially compensated for. Another point in favour of the usage of this particular combination of three datasets is the rather good concordance among them (see Fig. 1), which applies at least for the case of a constant w quintessence, and therefore seems a priori a property that will be shared by models with a dynamical EoS parameter.

2 OSCILLATING DARK ENERGY

2.1 Our parametrizations

We have just presented motivations for studying oscillating dark energy. In general, in order to infer conclusions about the dynamical behaviour of dark energy and its consequences in the expansion of the Universe, one has to make some concessions to try and make the best out of a collection of noisy scattered data. One of the most popular is to propose a parametric reconstruction obeying some basic requirements. Our proposal fits precisely in this kind of approach, and in order to examine the adequacy of oscillating patterns in the dark energy EoS we consider a simple and periodic phenomenological parametrization for the EoS, as proposed and studied in Linder (2006):

¹ This is the usual factor which relates pressure and density of any given component through the relation $w_X \doteq p_X/\rho_X$.

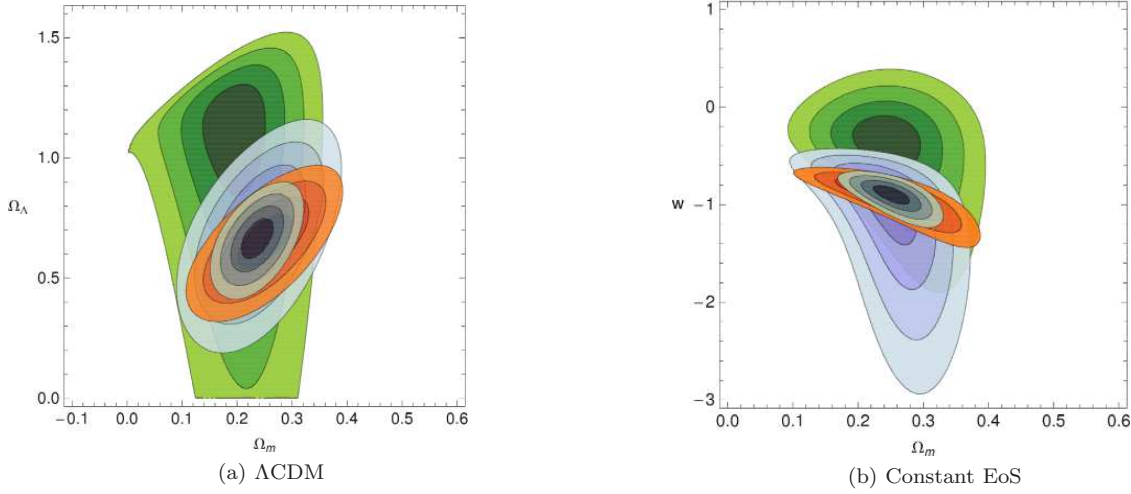


Figure 1. Credible intervals of the different observational data sets: *green* ones correspond to GRBs, *purple* to Hubble parameter data, *orange* to SNeIa and *blue* to the combination of all observational data. To construct these contour plots we have considered a prior on Ω_m and w_0 from WMAP-5years.

$$w(a) = w_c - A \sin(B \ln a - \Theta). \quad (1)$$

Equation (1) describes evolutionary dark energy with

- Θ being the phase of the oscillation, which for simplicity is assumed to be zero.
- w_c being the centre of the range over which $w(a)$ oscillates. In the $\Theta = 0$ case the parameter w_c is equal to the present value of the dark energy EoS, $w(a=1) = w_c = w_0$.
- A being the amplitude of the oscillations, which obviously must be non zero for a dynamical w . If this EoS is the effective realisation of a canonical scalar field, A should fulfil the constrain $w_0 - A \geq -1$; but we leave it completely free and let the observational data speak out its value.
- B is the frequency of the oscillations; and there are some key remarks to be made about it. In order to notice distinctly the presence of an oscillatory behaviour B should fulfil the condition

$$|B \ln a_{min}| > 2\pi, \quad (2)$$

where a_{min} is given by the highest redshift in the dataset. For our observational data this value is associated with a GRB at $z = 5.6$, for which we infer the constraint $B > 3.3$. Nevertheless, as SNeIa represent by far the dataset with the largest statistical power in our analysis and they span a smaller redshift range, it seems reasonable that an oscillating pattern will be only detectable for larger values of B .

Previous works have attempted to set constraints in these parameters but they have not been able to distinguish an oscillatory model from one with a constant EoS. This is partly due to the data sets employed, but also because of excessive restrictions on the parameters.

In this new attempt at exploring oscillating dark energy we use a new combination of data sets so as to obtain more reliable constraints, but we also make a few other key changes: specifically we carry out an analysis for a discrete set of fixed B values to try and avoid the arbitrariness in the choice of this parameter present in works by other authors.

In addition, and given the lack of grounds for very strong restrictions on phenomenological parametrizations of dark energy we have analysed two more models which rep-

resent a slight departure from the perhaps excessively nicely shaped trigonometric parametrization by Linder. Our first proposal in this direction is

$$w(a) = w_c - A J_1(B \ln a - \Theta), \quad (3)$$

where again we have set the phase $\Theta = 0$ so that $w_c = w_0$, and J_n is the Bessel function of the first kind with $n = 1$. The Bessel function $J_1(x)$ shows oscillations which are damped with growing x , as opposed to the constant amplitude of the trigonometric case. So in this case the EoS parameter w would have an oscillating trend modulated by a damping effect which makes the amplitude smaller and smaller as we go back in time (in the redshift space).

As we have to set observational constraints on parameters, we have to compute the Hubble factor

$$H^2(a) = \Omega_m a^{-3} + (1 - \Omega_m) a^{-3(1+\overline{w}(a))}, \quad (4)$$

which depends on the present value of the fractional matter density Ω_m , and on the averaged equation of state parameter

$$\overline{w}(a) = \frac{\int_0^{\ln(a)} w(a) d \ln(a)}{\ln(a)}. \quad (5)$$

So, we will work at some points with this expression of the EoS parameter instead of the usual one. It can be noticed that for the two parametrizations presented above, and we realised that the averaged forms follow a common pattern; the parametrization given by the Eq. 1 takes the form

$$\overline{w}(a) = w_0 + \frac{A}{B} \frac{\cos(B \ln a) - 1}{\ln(a)}, \quad (6)$$

whereas the parametrization given by Eq.3

$$\overline{w}(a) = w_0 + \frac{A}{B} \frac{J_0(B \ln a) - 1}{\ln(a)}. \quad (7)$$

With Eq. 7 and Eq. 6 as a reference, we propose another parametrization with a damped oscillating behaviour,

$$\overline{w}(a) = w_0 + \frac{A}{B} \frac{(\pi/2) H_{-1}(B \ln a) - 1}{\ln(a)} \quad (8)$$

where w_0 is the value of the EoS at present and H_{-1} is the Struve function, H_α , of order $\alpha = -1$. The Struve function lies between the trigonometric case, with constant amplitude, and the Bessel function, being less acutely damped than the Bessel function. It can be checked that the $w(a)$ function for this new proposal is an oscillating one as well, so this new model fits is the aim of the discussion.

Anyway, we have to underline that our three w models depend on $\ln a$ (i.e. $\ln(1+z)$) so these effects are quite smoothed and not so evident when depicted on even a large redshift interval such as the one limited by the re-ionisation one ($z = 1089$). However, such parametrizations, as first shown by Linder (2006), allow for analytical expressions of $H(z)$ (see Eq. 5) and thus result convenient for evaluation purposes.

Interestingly, as we will discuss later, the main consequences of an oscillating equation of state are more evident on the deceleration $q(z)$ function than on the Hubble function or the dark energy fractional density Ω_X .

2.2 Earlier Works

In Riess (2007) an interesting observational clue of a possible oscillating behaviour in the EoS was found. Fitting a quartic polynomial of $w(z)$ to SNeIa observations indications that such oscillations might be really present were found. Even though the redshift range where these oscillations seem to be present is actually rather small; these results motivated a plethora of works trying to analyse this possibility deeper.

In Xia (2005) the formulation

$$w(z) = w_0 + w_1 \sin(z), \quad (9)$$

was used to model a quintom scenario phenomenologically. The analysis was conducted using luminosity distances of SNeIa, the CMB shift parameter and the linear growth rate from large scale structure. Combining all these data sets the best fit values found were $w_0 = -1.33$, $w_1 = 1.47$. Such oscillating model differs very little from the linear one ($w(z) = w_0 + w_1 z$) when considering constraints from SNeIa only, and the oscillating case is only mildly preferred. This was somehow to be expected as for low redshifts the two parametrizations are very similar. Note that as in this study the oscillation frequency was fixed to a specific value we meet again the difficulties to make general inferences.

An extension of the latter was done in Xia (2006), where

$$w(a) = w_0 + w_1 \sin(w_2 \ln a + w_3), \quad (10)$$

was proposed, therefore now including also a period and a phase. One further degree of sophistication was introduced in the analysis as it was carried out using a modified version of CosmoMC so as to have into account dark energy perturbations. The results indicate that w_0 is acceptably well constrained, while w_1 is poorly constrained, and w_2 and w_3 can be regarded as completely unconstrained. This is not surprising, though, as highly dimensional parametrizations of dark energy seem to suffer this problem typically given the precision of observational data at present.

In Xia (2008) constraints on the cosmological parameters of some oscillating models were analysed using simulated data from future Planck measurements. Two different parametrizations of the dark energy EoS were used, the CPL one

$$w(a) = w_0 + w_1 (1 - a) \quad (11)$$

and the a reformulation of the Linder (2006) oscillating one,

$$w(a) = w_0 + w_1 \sin(w_2 \ln(a)), \quad (12)$$

having fixed the phase parameter to zero. In addition, one further choice was made: for simplicity and for focusing the analysis on low redshifts, the period parameter was fixed as $w_2 = 3\pi/2$ (because it corresponds to a period in the redshift range $0 < z < 2$ where data from supernovae are more robust). Then they use present data from WMAP3, ESSENCE SNeIa, SDSS (for details see reference) to derive best fit values for the EoS parameters which are assumed as the fiducial values for deriving constraints from Planck mission details. The following results were obtained:

$$w_0 = -1.03_{-0.15-0.26}^{+0.15+0.36}, \quad w_1 = -1.03_{-0.587-1.570}^{+0.562+0.781} \quad (13)$$

for the CPL EoS, and

$$w_0 = -0.981_{-0.340-0.748}^{+0.320+0.534}, \quad w_1 = -0.068_{-0.591-1.245}^{+0.561+1.037} \quad (14)$$

for the oscillating model.

Assuming the CPL EoS they are able to conclude that a Quintom scenario with a $w(z)$ which crosses the phantom divide is favoured against the Λ CDM scenario (it is mildly favoured with present data while future surveys can provide narrower constrains). Assuming the oscillating EoS the same conclusion can be derived, even if the constraints are weaker, and the low value for the amplitude of oscillation makes the constant $w(z)$ (i.e. Λ CDM model) equally possible.

For what concerns the oscillating model, these results are backed up in Liu (2009), where the following 68% CL values were obtained:

$$w_0 = -0.958 \pm 0.098, \quad w_{amp} = 0.030_{-0.130}^{+0.124} \quad (15)$$

From these results one can conclude that the EoS fit with current data provides as good as Λ CDM, and that the oscillation amplitude is limited: $|w_{amp}| < 0.232$ at 95%CL.

An oscillating model different from the one proposed by Linder is analysed in Jain (2007) (inspired by a previous idea in Feng (2006)). The authors used SNeIa, the CMB shift parameter and the measurement of the BAO peak from SDSS in order to constrain the sine version of the oscillating EoS written in the form

$$w(a) = w_0 - A \sin(B \ln a) \quad (16)$$

and the alternative

$$w(a) = -\cos(b \ln a). \quad (17)$$

The period parameter b in the second model drives the accelerating/decelerating epochs, and in the limit of small b one has $w(a) \sim -1$.

Final results show that $b = 0.06 \pm 0.01$ at 1σ level, a value which is consistent with limits required by CMB and correct power spectrum and which represents a *clear* evidence for an oscillating behaviour with a very long period (i.e. small but clear deviation from cosmological constant).

Another interesting work is Kurek (2008), where many different EoS were compared with a Bayesian approach. They worked with the so called linear EoS, i.e. CPL model; with pure oscillating models, the cosine one, $w(z) = w_0 \cos(w_c \ln(1+z))$, and the sine one, $w(z) = -1 + w_0 \sin(w_s \ln(1+z))$; with a damped version of previous oscillating models, $w(z) = w_0(1+z)^3 \cos(w_c \ln(1+z))$ or

$w(z) = -1 + w_0(1+z)^3 \sin(w_s \ln(1+z))$; and with a more complicated version of the dark energy EoS directly derived from the dynamics of the phantom scalar field (see reference for details). Analysing the values of the Bayesian evidences obtained fitting data (SNeIa, CMB, BAO) for each particular model, and comparing them with the Jeffreys scale (Jeffreys (1961)), they concluded that there is a substantial evidence for preferring pure oscillating model (sine) and the one derived from phantom field dynamics over the linear one, while damped versions are completely excluded. In addition, they found no strong evidence to favour Λ CDM over the oscillating models.

As stated in the Introduction, completely different approaches are possible as well; for example, in Sáez (2009) the starting point was an oscillating model for $H(z)$ instead of $w(z)$. Finally, it is possible to consider oscillating fields, which do not necessarily produce an oscillating EoS Frieman (1995).

3 OBSERVATIONAL DATA

We have tested the possible periodicity of the Hubble function by using three different observational data sets, i.e.:

- the reconstructed Hubble data given in Stern (2009);
- the *Constitution* Supernovae data set described in Hicken (2009);
- the Gamma Ray bursts luminosity distances measured and analysed in Kodama (2008).

3.1 Hubble parameter: Stern et al. 2009 data set

Recently in Stern (2009) an update of the Hubble function $H(z)$ data extracted from differential ages of passively evolving galaxies previously published in Simon (2005) was presented. Constraining the background evolution of the Universe using these data is interesting for several reasons. Firstly, they can be used together with other cosmological tests in order to get useful consistency checks or tighter constraints on models. Secondly, and more importantly, in contrast to standard candle luminosity distances or standard ruler angular diameter distances, the Hubble function is not integrated over. This is a key point because if a periodic behaviour is present in $w(a)$ it should be directly detectable in $H(a)$ while it could be lost in luminosity or angular diameter distances because of integration stages.

The Hubble parameter dependence on the differential age of the Universe in terms of redshift is given by

$$H(z) = -\frac{1}{1+z} \frac{dz}{dt}. \quad (18)$$

Thus, $H(z)$ can be determined from measurements of dt/dz . As reported in Jiménez (2002), Jiménez (2003), Simon (2005) and Stern (2009), values of dt/dz can be computed using absolute ages of passively evolving galaxies.

The galaxy spectral data used by Stern (2009) come from observations of bright cluster galaxies done with the Keck/LRIS instrument². The purposely planned Keck-

survey observations have been extended with other datasets: SDSS improvements in calibration available in the Public Data Release 6 (DR6) have been applied to data in Jiménez (2003); the SPICES infrared-selected galaxies sample in Stern (2000); and the VVDIS survey by the VLT/ESO telescope in Le Fevre (2005).

The authors of these references bin together galaxies with a redshift separation which is small enough so that the galaxies in the bin have roughly the same age; then, they calculate age differences between bins which have a small age difference which is at the same time larger than the error in the age itself (Stern (2009)). The outcome of this process is a set of 11 values of the Hubble parameter versus redshift. A particularly nice feature of this test is that the sensitivity of differential ages to systematic error is lower than in the case of absolute ages (Jiménez (2004)).

Observed values of $H(z)$ can be used to estimate DE parameters by minimising the quantity

$$\chi_H^2(H_0, \{\theta_i\}) = \sum_{j=1}^9 \frac{(H(z_j; \{\theta_i\}) - H_{obs}(z_j))^2}{\sigma_H^2(z_j)} \quad (19)$$

where $H_0 \doteq 100h$ will be fixed as $h = 0.742$ (Riess (2009)), while the vector of model parameters, θ_i , will be $\theta_i = (\Omega_m, w_0, A, B)$.

3.2 Supernovae: Hicken et al. 2009 data set

We use one of the most recent SNeIa samples, the *Constitution* sample described in Hicken (2009), which is a data set obtained by combining the Union data set by Kowalski (2008) with new 90 nearby objects from the CfA3 release described in Hicken (2009A).

The Union SNe compilation is a data set of low-redshift nearby-Hubble-flow SNe and is built with new analysis procedures for working with several heterogeneous SNeIa compilations. It includes 13 independent sets with SNe from the SCP, High- z Supernovae Search (HZSNS) team, Supernovae Legacy Survey and ESSENCE Survey, the older data sets, as well as the recently extended data set of distant supernovae observed with HST. After various selection cuts were applied in order to create a homogeneous and high-signal-to-noise data set, a final collection of 307 SNeIa events distributed over the redshift interval $0.15 \leq z \leq 1.55$ was obtained.

The CfA3 data set was originally made of 185 multi-band optical SNeIa light curves obtained at the F.L. Whipple Observatory of the Harvard-Smithsonian Center for Astrophysics (CfA); 90 of the original 185 objects passed the quality cuts of Kowalski (2008) and were added to the Union data set to form the Constitution one.

The statistical analysis of the Constitution SNe sample rests on the definition of the modulus distance,

$$\mu(z_j) = 5 \log_{10}[d_L(z_j, \{\theta_i\})] + \mu_0, \quad (20)$$

where $d_L(z_j, \{\theta_i\})$ is the Hubble free luminosity distance

$$d_L(z, \{\theta_i\}) = (1+z) \int_0^z dz' \frac{1}{H(z', \{\theta_i\})}. \quad (21)$$

The best fits to be presented will be obtained by minimising the quantity

² See Stern (2009B) for a detailed description of the observations, reductions and the catalog of all the measured redshifts

$$\chi_{\text{SN}}^2(\mu_0, \{\theta_i\}) = \sum_{j=1}^{397} \frac{(\mu(z_j; \mu_0, \{\theta_i\}) - \mu_{\text{obs}}(z_j))^2}{\sigma_{\mu}^2(z_j)} \quad (22)$$

where the σ_{μ}^2 are the measurement variances. The nuisance parameter μ_0 encodes the Hubble parameter and the absolute magnitude M , and has to be marginalised over. Giving the heterogeneous origin of the Constitution data set, and the procedures described in Kowalski (2008) and Hicken (2009) for reducing data, we have worked with an alternative version of Eq. (22), which consists in minimizing the quantity

$$\tilde{\chi}_{\text{SN}}^2(\{\theta_i\}) = c_1 - \frac{c_2}{c_3} \quad (23)$$

with respect to the other parameters. Here

$$c_1 = \sum_{j=1}^{307} \frac{(\mu(z_j; \mu_0 = 0, \{\theta_i\}) - \mu_{\text{obs}}(z_j))^2}{\sigma_{\mu}^2(z_j)}, \quad (24)$$

$$c_2 = \sum_{j=1}^{307} \frac{(\mu(z_j; \mu_0 = 0, \{\theta_i\}) - \mu_{\text{obs}}(z_j))}{\sigma_{\mu}^2(z_j)}, \quad (25)$$

$$c_3 = \sum_{j=1}^{307} \frac{1}{\sigma_{\mu}^2(z_j)}. \quad (26)$$

It is trivial to see that $\tilde{\chi}_{\text{SN}}^2$ is just a version of χ_{SN}^2 , minimised with respect to μ_0 . To that end it suffices to notice that

$$\chi_{\text{SN}}^2(\mu_0, \{\theta_i\}) = c_1 - 2c_2\mu_0 + c_3\mu_0^2 \quad (27)$$

which clearly becomes minimum for $\mu_0 = c_2/c_3$, and so we can see $\tilde{\chi}_{\text{SN}}^2 \equiv \chi_{\text{SN}}^2(\mu_0 = 0, \{\theta_i\})$. Furthermore, one can check that the difference between χ_{SN}^2 and $\tilde{\chi}_{\text{SN}}^2$ is negligible.

3.3 GRBs: Kodama et al. 2008 data set

The GRBs sample, described in Kodama (2008), is made of 33 GRBs within the redshift interval $z < 1.62$ and 30 GRBs in the redshift interval $1.8 < z < 5.6$. It is well known that GRBs are not standard candles as SNeIa; at the same time they contain a lot of important information about high redshift properties of the universe which cannot be derived from SNeIa. So their combined use can bring important and complementary information about the reconstruction of dark energy and gives us the possibility to detect eventually traces of an oscillatory behaviour on a larger redshift range. The calibration of GRBs data can be done in several ways, and many empirical formulas have been given for describing the peak energy-peak luminosity correlation. In Kodama (2008) the peak energy-peak luminosity correlation is described by the so called *Yonetoku relation*³ of the GRBs sub-sample in redshift interval $z < 1.62$ is calibrated without assuming any cosmological model and using the luminosity distance of the objects considered it is estimated from those of SNeIa with redshift $z < 1.755$. The calibrated Yonetoku relation is then finally applied to the high redshift GRBs sub-sample with redshift in the interval $1.8 < z < 5.6$. Final data consist of a set of calibrated luminosity distances, so that we can define the contribution to the total chi-square as:

$$\chi_{\text{GRB}}^2(\{\theta_i\}) = \sum_{j=1}^{63} \frac{(d_L(z_j; \{\theta_i\}) - d_L^{\text{obs}}(z_j))^2}{\sigma_{d_L}^2(z_j)} \quad (28)$$

where the $\sigma_{d_L}^2$ are the measurement variances.

4 STATISTICS AND DATA ANALYSIS

We will explore the probability distributions of our problem with Markov Chain Monte Carlo (MCMC) methods. These methods (fully described in Berg (2004), MacKay (2002), Neal (1993) and references therein) extract samples sequentially using a probabilistic algorithm (we have chosen the Metropolis-Hastings algorithm which we describe below) based on the Bayesian statistical approach. The main problem when running a Markov chain concerns how to avoid biased inferences or underestimations on errors of the theoretical parameters. The *problem of the convergence* is the main one among the problems of that sort, and it can be formulated as follows: how can one be sure that the properties of a sample from the MCMC algorithm are a good representation of the unknown distribution to be explored? In the following we discuss the details algorithm and the solution adopted for convergence.

4.1 Markov Chain algorithm and convergence test

The Metropolis-Hastings algorithm works as follows: starting from an initial parameter vector \mathbf{p} (in our case $\mathbf{p} = (\Omega_m, w_0, A, B)$), one generates a new trial point \mathbf{p}' from a *proposal density* $q(\mathbf{p}', \mathbf{p})$, which represents the conditional probability to have \mathbf{p}' given \mathbf{p} . This new point is accepted with probability

$$\alpha(\mathbf{p}, \mathbf{p}') = \min \left\{ 1, \frac{P(\mathbf{p}'|\mathbf{d})q(\mathbf{p}, \mathbf{p}')}{P(\mathbf{p}|\mathbf{d})q(\mathbf{p}', \mathbf{p})} \right\} \quad (29)$$

where $P(\mathbf{p}|\mathbf{d})$ is the conditional probability to have the parameter set \mathbf{p} given the observational data \mathbf{d} . Then, from Bayes' theorem it follows that this probability is:

$$P(\mathbf{p}|\mathbf{d}) \propto L(\mathbf{d}|\mathbf{p})P(\mathbf{p}) \quad (30)$$

with $L(\mathbf{d}|\mathbf{p})$ being the likelihood function containing information from the data, and $P(\mathbf{p})$ the prior on the parameters which contains all the supposed information on them before observing the data. If the chain moves to the new set \mathbf{p}' , then one says that it has been accepted, otherwise it has been rejected.

We choose the prior depending on the physical requirements a given parameter has. The proposal density is typically a Gaussian symmetric with respect to the two vectors \mathbf{p} and \mathbf{p}' , namely $q(\mathbf{p}, \mathbf{p}') \propto \exp(-\Delta p^2/2\sigma_T^2)$, with $\Delta \mathbf{p} = \mathbf{p} - \mathbf{p}'$, so that, from the detailed balance equation, we know that the final probability distribution is stationary under the Markov process. An important quantity in the testing proposal distribution is its dispersion σ_T ; as we will discuss below, we decide not to take a fixed value for it, but instead, we let it depend on the value of the parameters at any step.

One can say that a chain has reached convergence when the statistical properties of the extracted samples can describe the statistical properties of the unknown probability

³ See Yonetoku (2004)

distribution with *good accuracy*. Probability theory says that Markov processes will reach the exact final distribution in an asymptotic way, which means a sample's length will become infinite in an infinite computation time. Of course, as one is forced to operate with finite length samples, the question arises of how this truncation can bias the final statistical results, and if there are any parameters that can be able to give information about the goodness of the process. In the literature the most used parameter for this task is the *convergence ratio* (see Dunkley (2005)), defined as

$$r = \frac{\sigma_x^2}{\sigma_0^2}. \quad (31)$$

This is the ratio between the variance of the mean of the samples and the variance of the underlying unknown distribution (we will operate with standard distributions so that $\sigma_0^2 = 1$). Then r is required to be below a cut-off limit value, typically 0.01, to have a guaranteed convergence of the chain. This parameter is used in other convergence tests, such as the Gelmann-Rubin test (see Gelman & Rubin (1992)), which runs many parallel multiple chains and estimates r at any step; but we regard it a time and hardware expensive test.

An alternative solution to this problem in the spectral analysis approach proposed by Dunkley (2005). Is it clear that all the steps in MCMC are correlated; this correlation is somewhat intrinsic to the code, at least before having reached convergence, but it depends also on the value of σ_T^4 . But what is even more important is the behaviour of the correlation when the convergence has been reached: in this case the MCMC will sample from the underlying distribution and it will work like a random sampler, so that there will be no correlations in this regime.

This is the key idea of the test by Dunkley (2005): if we take the *power spectra* of the MCMC samples, we will have a large correlation on small scales, but the spectrum will become flat (like a white noise spectrum) when convergence has been reached. Then, checking the spectrum of just one chain (instead of many parallel chains as in Gelmann-Rubin's test) will be sufficient to assess that convergence has indeed been reached. We will give just a short account of the steps to be followed to implement the test, but for a more detailed reference see Dunkley (2005).

In brief, we calculate the discrete power spectrum of the chains,

$$P_j = |a_N^j|^2, \quad (32)$$

with

$$a_N^j = \frac{1}{\sqrt{N}} \sum_{n=0}^{N-1} x_n \exp \left[i \frac{2\pi j}{N} n \right], \quad (33)$$

where N and x_n are respectively the length and a given element of the sample from the MCMC, $j = 1, \dots, N/2 - 1$, and the wave number k_j of the spectrum is related to the index j by the relation $k_j = 2\pi j/N$. Then we fit it to an analytical template:

$$P(k) = P_0 \frac{(k^*/k)^\alpha}{1 + (k^*/k)^\alpha}, \quad (34)$$

or in equivalent logarithmic form:

$$\ln P_j = \ln P_0 + \ln \left[\frac{(k^*/k_j)^\alpha}{1 + (k^*/k_j)^\alpha} \right] - \gamma + r_j, \quad (35)$$

where $\gamma = 0.57216$ is the Euler-Mascheroni number and r_j are random measurement errors with $\langle r_j \rangle = 0$ and $\langle r_i r_j \rangle = \delta_{ij} \pi^2/6$. The fit provides estimates of three parameters, but only two of them are fundamental to our analysis. The first one is P_0 , which is the value of the power spectrum extrapolated for $k \rightarrow 0$; this is an important parameter because from it we can derive the convergence ratio using $r \approx P_0/N$. The second important parameter is j^* (the index corresponding to k^*), which is related to the turnover point from a power to a flat spectrum; the estimated value of j^* has to be $\gtrsim 20$, so one can be sure that the number of points in the sample coming from the convergence region are larger than the number of noisy points. If these two conditions are met for all the parameters, then the chain has reached convergence, and the statistics from the MCMC procedure describes well the underlying probability distribution. Following the advise in Dunkley (2005) we perform the fit over the range $1 \leq j \leq j_{max}$, with $j_{max} \sim 10j^*$, where a first estimation of j^* can be obtained from a fit with $j_{max} = 1000$, and then perform a second (or even a third) iteration to have a better estimation of it.

4.2 Model selection tests

After having estimated the value of the parameters set by using the MCMC approach, we need a tool for comparing, selecting and testing the statistical goodness of our results. The related literature is too extensive for being reviewed here, so we will only refer in some detail to the tools we have chosen.

Since the MCMC technique is based on a Bayesian approach, the best way for comparing models is arguably the Bayesian Evidence. It is defined as

$$E \equiv \int \mathcal{L}(\theta) P(\theta) d\theta, \quad (36)$$

where \mathcal{L} is the likelihood function, θ is the parameters vector and $P(\theta)$ is the prior distribution for the parameters. It is clear from its definition, that the evidence of a model is the average likelihood of the model with respect to the prior: models which fit the data well and make narrow predictions are likely to fit well over much of their available parameter space, giving a high evidence. So using evidence for comparing models is a very appropriate task. Model comparison requires defining then Bayes factor,

$$B_{ij} = \frac{E(M_i)}{E(M_j)}, \quad (37)$$

which is the ratio between the evidence values of two models, M_i and M_j . If $B_{ij} > 1$ then the model M_i is preferred with respect to the model M_j . By convention, Bayes factor is judged on the Jeffreys' scale (Jeffreys (1961)): for $1 < \ln B_{ij} < 2.5$ there is a "substantial" evidence in favour of the model with the greatest Bayesian evidence; for $\ln B_{ij} > 5$ the evidence is "decisive".

Moreover, we have to underline in favour of the Bayesian evidence, that it is a full implementation of Bayesian inference and can be directly interpreted in terms

⁴ For a detailed analysis of this aspect see Dunkley (2005)

of model probabilities. Unfortunately, being a highly-peaked multi-dimensional integral, its estimation typically requires a hard and challenging numerical effort. Even if some algorithms have been found which simplify this operation, it is always preferable to have easier tools for estimating it and comparing models.

The easiest and most used tools are different versions of the Information Criteria. Generally, the introduction of a higher number of parameters improves the fit to the chosen dataset, regardless of whether or not these new parameters are really relevant. As a consequence, the simple comparison of the maximum likelihood value of different models will tend to favour the model with the highest number of parameters. The information criteria work just in this direction: they compensate this behaviour by penalising models which have more parameters.

The first test is the Akaike Information Criterion (AIC) defined as

$$\text{AIC} = -2 \ln \mathcal{L} + 2k \quad (38)$$

where \mathcal{L} is the maximum likelihood value and k is the number of parameters of the model (Akaike (1974)). The AIC is derived by an approximation of the Kullback-Leibler information entropy, which measures the difference between the true data distribution and the model one (Burnham & Anderson (2002) and Takeuchi (2000)). The best model is the one which minimises the AIC, and no requirement for the models is asked for.

There also exists an AIC version for small sample sizes, the corrected AIC, AIC_c (Burnham & Anderson (2002)) given by

$$\text{AIC}_c = \text{AIC} + \frac{2k(k+1)}{N-k-1}, \quad (39)$$

where N is the number of points in the dataset. Since the correction term disappears for large sample sizes, $N \gg k$, we will use this last definition for comparing models (as pointed out in Liddle (2007), it is always preferable to use the corrected version rather than the original one).

From the same principles of AIC (minimisation of the Kullback-Leibler information entropy) another comparing tool can be derived, the Residual Information Criterion (RIC). We will use the corrected version in Leng (2007), where the RIC_c is defined as

$$\text{RIC}_c = -2 \ln \mathcal{L} + (k-1) + \frac{4k}{N-k-1}. \quad (40)$$

When $N \gg k$, RIC_c has a smaller penalty than AIC_c .

Generally, when $\Delta \text{AIC} \gtrsim 1$, it follows that the two models are significantly different, and the one with the lowest value of AIC is the preferred one. Finally, we have to keep in mind that AIC tends to favour models with a high number of parameters and it is “dimensionally inconsistent”, namely, that even as the dataset size tends to infinity, the probability of the AIC incorrectly picking an overparametrized model does not tend to zero (Liddle (2004) and references therein). Let us thus consider alternatives.

The Bayesian Information criterion (BIC) was introduced in Schwarz (1978) and is defined as

$$\text{BIC} = -2 \ln \mathcal{L} + k \ln N. \quad (41)$$

Again in this case the best model has the lowest BIC, and it is clear from this expression that BIC penalises models with

a high number of parameters more than AIC. Being the BIC a good approximation for twice the log of the Bayes factor, it can be compared with Jeffreys’ scale, so that $\Delta \text{BIC} > 5$ means a “strong” evidence in favour of the model with lowest BIC values, while for $\Delta \text{BIC} > 10$ this evidence is “decisive”.

We will also use the Deviance information criterion (DIC) of Spiegelhalter (2002), which mixes elements from both Bayesian and information theory. It is well suited to our case because it is easily computable from posterior samples such as those coming from MCMC runs. It relies on the definition of the effective number of parameters, p_D , also known as the Bayesian complexity. It is defined as

$$p_D = \overline{D(\theta)} - D(\bar{\theta}), \quad (42)$$

where

$$D(\theta) = -2 \ln \mathcal{L}(\theta) + C \quad (43)$$

with C a constant which vanishes from any derived quantity, and the chi-square defined as usual as $\chi^2 = -2 \ln \mathcal{L}$. This definition shows that p_D can be considered as the mean deviance minus the deviance of the means, and this is the key quantity in estimating the degrees of freedom of a test. Finally the DIC is defined by

$$\text{DIC} = D(\bar{\theta}) + 2p_D = \overline{D(\theta)} + p_D \quad (44)$$

where one can recognise a similar-to-AIC formulation in the first expression, while a Bayesian definition and measure of model adequacy (penalised by an additional term related to the model dimensionality) is implicit in the second one. The DIC is also useful for another reason: it overcomes the difficulties AIC and BIC have to discount parameters which are unconstrained by data (BIC is of even more suspicious validity when there is any parameter degeneracy). Finally, DIC (like BIC) is not dimensionally inconsistent, so it is able to detect wrong high dimensionality parametrizations.

5 CONSTRAINTS AND ASSUMPTIONS

We have implemented a few priors for running our MCMCs. The main one has been to set the control $0 < \Omega_m < 1$, which is a minimum physicality requirement. We have also set mild Gaussian priors on Ω_m and w_0 with the 3σ error bar from WMAP5 as a reference.

As we stated in the previous sections it would be possible to set physical limits on the parameters of the oscillating model, such as A and B . The amplitude A should have a value which depends on the theoretical scenario chosen to be the fiducial one. In the case of ΛCDM , one could require that the minimum value for the EoS was $w_0 - A \geq -1$. But it is clear that with this case will exclude the possibility of a phantom behaviour, which is a possibility present data do not rule at and in some cases seem to be the preferred one. For that reason regard leaving A free as the best option.

At the same time, the frequency (period) parameter B should be subject to $|B \ln a_{\min}| > 2\pi$. The highest redshift of our observational data corresponds to a GRB observation at $z = 5.6$. For that choice, B should be $B > 3.3$. Anyway, we have no a priori strong clues about the validity of a periodic oscillating EoS, so there is scarce guidance regarding a suitable lower bound on B . We could have oscillations with

a period bound given by the highest redshift in the supernovae data, so in this case we would have $B > 5.7$; or we could have no detectable oscillations at all in our redshift range so that a really small value of B could turn out to be the best fit. In addition, rigorously the bound on B we are commenting about (proposed by Linder) makes only sense for the sine oscillating model, which has a valid definition for the *oscillation period* and not for other two models. Anyway, also in this cases the B parameters can be related to periodic properties of the dark EoS parameter, so we treated it on the same footing in the analysis of the three models.

There is also another problem concerning the number of free parameters one introduces in a model. In our case we would have a dark energy EoS with three free parameters, namely w_0 , A and B (which become four parameters because of the presence of Ω_m in the expression for the Hubble function and luminosity distance). This poses a well known problem in reconstructing or modeling the EoS with parametric relations: how many parameters can we enquire about? Following the Occam's razor prescription one could be tempted to choose the minimalistic option: models with few parameters are the best ones. But sometimes this could be a not *physically* good choice: complex systems could require complex analytical formulas and a large number of parameters could describe a more suitable behaviour of dark energy. It is also possible that not all the introduced parameters are really free, and there is a correlation/dependence between some of them; but this cannot be known a priori when proposing a new model.

The only solution is to decide depending on the physical problem one has to face with. In preliminary runs we left all the parameters free, but it soon emerged that there is a strong degeneracy between some of them, mainly between A and B . While Ω_m and w_0 were well constrained, the two main parameters of our oscillating models showed a degeneracy which made them eventually unconstrained and yielded no satisfactory information about our proposed EoS.

So we turned to another way to proceed: we fixed the value of B to a set of discrete values scanning entirely the range of values which could potentially lead to detectable oscillations of our observable functions given the criteria discussed above.

6 RESULTS

Tables 1, 2 and 3 summarize our results. As ours is a more exhaustive analysis than previous ones in the literature it is clear that we can draw stronger conclusions. The main one is that the current data do not seem to give as strong constraints on A as on the other parameters Ω_m and w_0 , but a clear trend in A can be guessed, which becomes quite evident in Fig. 6. A fit of A as a function of B using a linear relation turns out to be the best one for the sine model; whereas, for the Bessel and Struve function a quadratic relation is preferred.

If we pay attention to the behaviour of w_0 , which is present value of EoS, we see that is very well constrained. There is a slight difference between the sine and the Bessel or Struve cases, but in all cases we can exclude phantom like behaviour at 1σ level (the prior does not in principle hinder it as it rather weak). In Fig.6, we can see that the

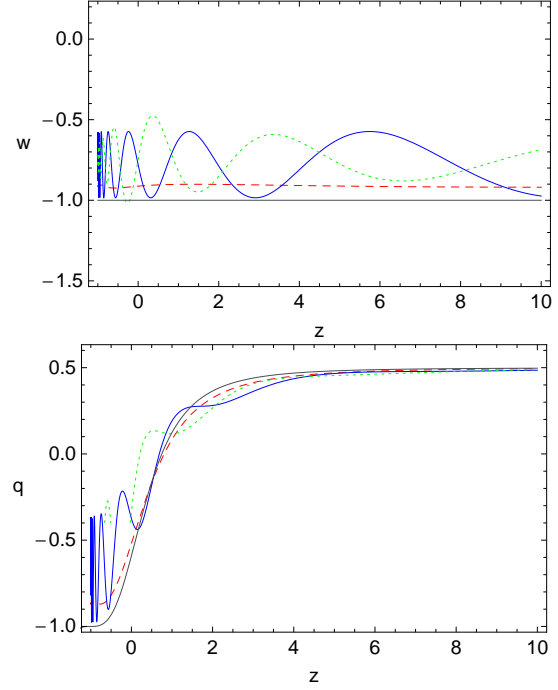


Figure 2. In these figures we plot the redshift-variation of the EoS and the acceleration for the best values of the parametrizations. The colors have the same meaning of Figs. (2).

Table 1. Averaged EoS: $\bar{w}(a) = w_0 + \frac{A}{B} \frac{\cos(B \ln a) - 1}{\ln(a)}$.

B	χ^2_{red}	z_{min}	Ω_m	A	w_0
$\frac{\pi}{2}$	1.0787	53.59	$0.25^{+0.02}_{-0.02}$	$0.23^{+0.37}_{-0.53}$	$-0.95^{+0.13}_{-0.12}$
$\frac{2\pi}{3}$	1.0797	19.09	$0.25^{+0.02}_{-0.02}$	$0.04^{+0.38}_{-0.37}$	$-0.91^{+0.12}_{-0.13}$
$\frac{5\pi}{6}$	1.0796	10.02	$0.25^{+0.02}_{-0.02}$	$0.10^{+0.30}_{-0.35}$	$-0.93^{+0.13}_{-0.14}$
π	1.0799	6.39	$0.25^{+0.02}_{-0.02}$	$0.07^{+0.34}_{-0.38}$	$-0.93^{+0.17}_{-0.17}$
$\frac{7\pi}{6}$	1.0803	4.55	$0.26^{+0.02}_{-0.02}$	$-0.08^{+0.34}_{-0.41}$	$-0.86^{+0.21}_{-0.16}$
$\frac{4\pi}{3}$	1.0802	3.48	$0.25^{+0.02}_{-0.02}$	$-0.14^{+0.35}_{-0.36}$	$-0.84^{+0.22}_{-0.19}$
$\frac{3\pi}{2}$	1.0794	2.79	$0.25^{+0.02}_{-0.02}$	$-0.18^{+0.30}_{-0.34}$	$-0.80^{+0.21}_{-0.17}$
$\frac{5\pi}{3}$	1.0788	2.32	$0.25^{+0.02}_{-0.02}$	$-0.21^{+0.30}_{-0.27}$	$-0.78^{+0.17}_{-0.20}$
$\frac{11\pi}{6}$	1.0783	1.98	$0.25^{+0.02}_{-0.02}$	$-0.21^{+0.26}_{-0.22}$	$-0.78^{+0.14}_{-0.19}$

Table 2. Averaged EoS: $\bar{w}(a) = w_0 + \frac{A}{B} \frac{J_0(B \ln a) - 1}{\ln(a)}$.

B	χ^2_{red}	z_{min}	Ω_m	A	w_0
$\frac{\pi}{2}$	1.0806	53.39	$0.25^{+0.02}_{-0.02}$	$-0.11^{+1.00}_{-0.93}$	$-0.89^{+0.13}_{-0.14}$
$\frac{2\pi}{3}$	1.0801	19.09	$0.25^{+0.02}_{-0.02}$	$-0.02^{+0.82}_{-0.81}$	$-0.91^{+0.14}_{-0.13}$
$\frac{5\pi}{6}$	1.0801	10.02	$0.26^{+0.02}_{-0.02}$	$-0.00^{+0.60}_{-0.60}$	$-0.90^{+0.12}_{-0.13}$
π	1.0818	6.39	$0.26^{+0.02}_{-0.02}$	$-0.20^{+0.69}_{-0.63}$	$-0.86^{+0.15}_{-0.14}$
$\frac{7\pi}{6}$	1.0809	4.55	$0.25^{+0.02}_{-0.02}$	$-0.19^{+0.67}_{-0.55}$	$-0.86^{+0.15}_{-0.17}$
$\frac{4\pi}{3}$	1.0807	3.48	$0.26^{+0.02}_{-0.02}$	$-0.20^{+0.59}_{-0.67}$	$-0.85^{+0.18}_{-0.17}$
$\frac{3\pi}{2}$	1.0816	2.79	$0.26^{+0.02}_{-0.02}$	$-0.55^{+0.70}_{-0.66}$	$-0.73^{+0.21}_{-0.22}$
$\frac{5\pi}{3}$	1.0808	2.32	$0.26^{+0.02}_{-0.02}$	$-0.58^{+0.66}_{-0.62}$	$-0.71^{+0.20}_{-0.23}$
$\frac{11\pi}{6}$	1.0807	1.98	$0.25^{+0.02}_{-0.02}$	$-0.75^{+0.63}_{-0.56}$	$-0.65^{+0.19}_{-0.23}$

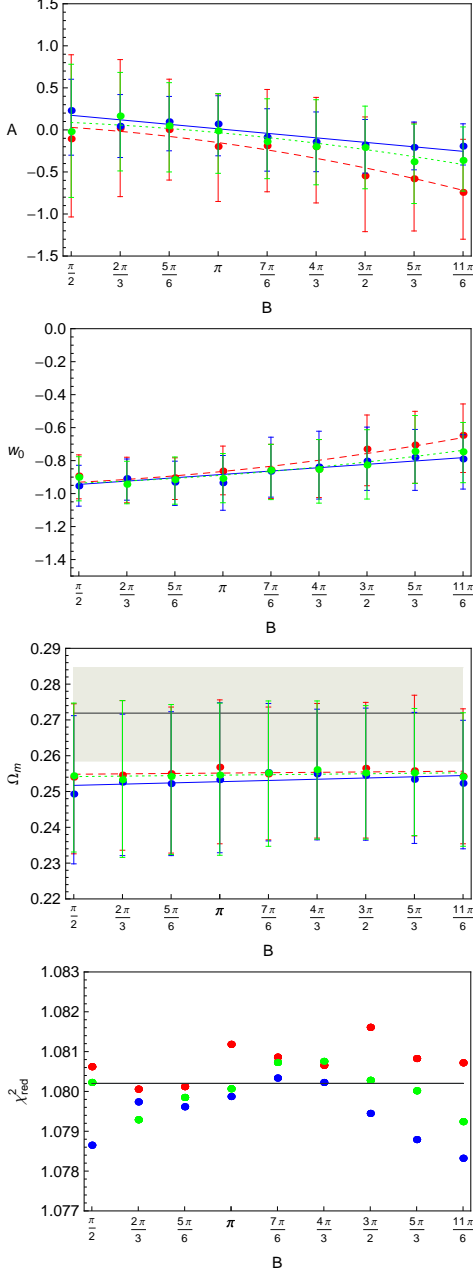


Figure 3. In these figures we plot the free parameters Ω_m , A , w_0 and the reduced χ^2 value versus the fixed B value for the different models. The blue points refer to the sine model (Eq.(6)); the red ones to the Bessel model (Eq.(7)), and the green ones to the Struve model (Eq.(8)). The gray line in Fig. 6 and Fig. 6 corresponds to Λ CDM values. In Fig. 6 the gray region indicates the values of Ω_m within 1σ error that describe Λ CDM.

behaviour for w_0 as a function of B agrees with the tendency of the amplitude A : as B grows the value of A becomes more negative so w_0 moves to less negative values, see Eq.3 and Eq.1. If we explore by means of fits how w and B are related, we find the same pattern as for A , the linear fit is preferred for the EoS with a sine form, and the quadratic one for the EoS with the Bessel or Struve function.

The remaining parameter, Ω_m , is very well constrained

Table 3. Averaged EoS: $\overline{w}(a) = w_0 + \frac{A}{B} \frac{(\pi/2)H_{-1}(B \ln a) - 1}{\ln(a)}$.

B	χ^2_{red}	z_{min}	Ω_m	A	w_0
$\frac{\pi}{2}$	1.0802	53.39	$0.25^{+0.02}_{-0.02}$	$-0.02^{+0.80}_{-0.78}$	$-0.90^{+0.12}_{-0.14}$
$\frac{2\pi}{3}$	1.0793	19.09	$0.25^{+0.02}_{-0.02}$	$0.17^{+0.52}_{-0.55}$	$-0.94^{+0.12}_{-0.14}$
$\frac{5\pi}{6}$	1.0798	10.02	$0.25^{+0.02}_{-0.02}$	$0.05^{+0.51}_{-0.55}$	$-0.91^{+0.14}_{-0.15}$
π	1.0801	6.39	$0.25^{+0.02}_{-0.02}$	$0.01^{+0.44}_{-0.50}$	$-0.91^{+0.15}_{-0.15}$
$\frac{7\pi}{6}$	1.0807	4.55	$0.26^{+0.02}_{-0.02}$	$-0.14^{+0.51}_{-0.44}$	$-0.86^{+0.16}_{-0.18}$
$\frac{4\pi}{3}$	1.0808	3.48	$0.26^{+0.02}_{-0.02}$	$-0.20^{+0.56}_{-0.45}$	$-0.84^{+0.18}_{-0.20}$
$\frac{3\pi}{2}$	1.0803	2.79	$0.26^{+0.02}_{-0.02}$	$-0.21^{+0.49}_{-0.49}$	$-0.83^{+0.21}_{-0.21}$
$\frac{5\pi}{3}$	1.0800	2.32	$0.26^{+0.02}_{-0.02}$	$-0.38^{+0.45}_{-0.50}$	$-0.74^{+0.22}_{-0.18}$
$\frac{11\pi}{6}$	1.0792	1.98	$0.25^{+0.02}_{-0.02}$	$-0.36^{+0.39}_{-0.36}$	$-0.75^{+0.18}_{-0.19}$

and fully agrees with literature expected values, being $\Omega_m \simeq 0.25$ and this value changes negligibly with B , see Fig.6.

So, with the current data it seems that B cannot be really constrained, that is, all B values seem to be of similar statistical validity. We have a very slight preference for values which are different from those chosen by other authors. Generally the chosen value is $B = 3\pi/2$ as corresponds to the typical supernovae redshift range. In our analysis the lowest value of for chi-square does not correspond to that value of B ; for the sine and Struve models the minimum is for $B = 11\pi/6$ which means that we can detect oscillations within a redshift $z \sim 1.98$, comprised by our data. For the Bessel oscillating model we have a chi-square minimum value at $B = 2\pi/3$ which will need a redshift $z \sim 19.09$, which is outside of our observational data range. Fig. 2 reflects clearly these behaviours: the best values, from the statistical point of view, for the sine and Struve models depend allow us to detect a complete oscillation in the range of our observational data.

Nevertheless, focusing our attention on Fig. 6, we can see that for almost all the values of the frequency, B , the values of chi-square of the sine parametrization are smaller than those of others parametrizations. If we take this into account and the fact that the best value of this parametrization corresponds to a $B = 11\pi/6$, we could say that observational data shows a preference for a periodic EoS with a small period.

At the same time, if we look at the variation of the acceleration parameter (Fig.6) in the recent past we can observe that it has recently peaked and is slowing down at present as have been pointed in Shafieloo et al. (2009).

Moving to the statistical side of the analysis, we have to argue if the proposed models are reasonably good or not, and above all if they can compete with the concordance Λ CDM model. From our results we conclude an oscillating pattern in the dark energy is an admissible *possibility*, as there is so far no concluding evidence against it; and from some statistical perspectives they even represent a better option than its main competitor, Λ CDM. Tables 4 summarizes our findings on the statistical side.

If we take a look at the reduced chi-square values, we can see that all the models have lower values than the Λ CDM one, even if the differences are really small. In particular, the sine model seems the best one. If we take a look to the AIC_c values, we see that the sine model is just in a border line position if we consider the limit we discussed in Section 4.2, i.e. $\Delta\text{AIC} \gtrsim 1$. On the contrary, we should absolutely reject

Table 4. Statistical criteria

Model	χ^2	χ^2_{red}	ΔAICc	ΔBIC	ΔRICc	ΔDICc
ΛCDM	507.7003	1.0802	0	0	0	0
Sinus	504.6550	1.0783	0.9975	9.2687	-1.0282	1.9145
Bessel	505.4669	1.0801	1.8094	10.0806	-0.2163	2.0344
Struve	505.0848	1.0792	1.4273	9.6985	-0.5984	2.0023

the Bessel and Struve models. But the situation changes when considering RICc : we know that it has a small penalty than AICc when $N \gg k$ as it is in our case, where we have $N = 472$ and $k = 3$. And we see that its values favour the oscillating models with respect to ΛCDM ; they are even negative, meaning that the RICc of oscillating parametrizations are better.

The situation reverses again when moving to BIC ; if we compare the values obtained with the Jeffreys' scale, we should conclude that there is an *almost decisive* evidence against oscillating patterns. But we have to remember that BIC has some problem when facing degeneracies between parameters, like the behaviours of the amplitude and of w_0 seem to reflect.

These degeneracies would well be the reason of the “bad results” offered by BIC , which is also challenged by another criterion, DIC , which looks more favourable with oscillating dark energy. Since DIC relies also on the Bayesian approach, we can apply Jeffreys' scale to it in the same fashion as above, and from this we conclude there is not a significant evidence against oscillations.

7 CONCLUSIONS

In this paper we have performed a quite detailed analysis towards the detection of oscillating patterns in the dark energy EoS. We have considered different phenomenological models, starting from the original sine models and then introducing two new ones, based on the special functions. Those new models differ from the sine one mainly because they show a damped amplitude in the oscillations when moving into the past.

Compared to prior works devoted to oscillating dark energy we can highlight that fact that instead of fixing the frequency parameter to a particular value, we have explored a discrete set of frequency values.

We have also introduced novelty with respect of the datasets used, as we take direct measurements of the Hubble factor and GRB luminosity data, which are arguably two directions of improvement as the sensitivity to oscillating patterns gets increased and a wider redshift range comes into play. Our theoretical setup has been complemented with a detailed statistical analysis using different model selection tools.

Numerical results show that while parameters like the matter content, Ω_m and the present value of dark energy EoS, w_0 can be constrained very well, this is not true for the amplitude and the frequency. In particular, between the amplitude A and w_0 seems to be working a degeneracy that cannot be solved. About the frequency, we can say that chi-square values are not really in favour of a particular value, being all in a very narrow range. But the best values favour

values of the frequency which mean oscillation detectable inside the present redshift range of SNeIa.

The statistical analysis seems does not seem to provide such a conclusive answer as desirable, though we think that oscillations can be considered as a possible alternative to a ΛCDM model for addressing the well know problems it suffers from (as review in the Introduction). All but one (BIC) of the statistical criteria used considered here are keen to the possible detection of oscillations in the EoS, there is even one of them (RIC) which seems to favor an oscillating pattern against a cosmological constant.

ACKNOWLEDGEMENTS

We are grateful to D. Yonetoku for providing us the GRB data and to E. Komatsu and M. Hicken for useful comments. We also wish to thank IZO-SGI SGlker (UPV/EHU, MI-CINN, GV/EJ, ESF), and in particular E. Ogando and T. Mercero, for technical and human support. R.L., V.S. and I.S. are sustained by the Basque Government through grant GIU06/37. R.L. and I.S. have additional support from the Spanish Ministry of Science and Innovation through grant FIS2007- 61800.

REFERENCES

- Akaike, H. 1974, IEEE Trans. Auto. Control., 19, 716
- Astier, P. et al. 2006, A&A, 447, 31
- Bahcall, N.A. et al. 2003, ApJ, 585, 182
- Bahcall, N.A., Bode, P. 2003, ApJ, 588, 1
- Berg, B.A., *Markov Chain Monte Carlo Simulations and Their Statistical Analysis*, World Scientific Publishing Co. Pte. Ltd., Singapore
- Burnham, K., P., Anderson, D., R. 2002, *Model selection and multimodel inference*, 2nd ed., Springer-Verlag, New York
- Chevallier, M., Polarski, D. 2001, IJMPD, 10, 213
- Clocchiati, A. et al. 2006, ApJ, 642, 1
- Cole, S. et al. 2005, MNRAS, 362, 505
- Copeland E.J., Sami M., Tsujikawa S., 2006, Int. J. Mod. Phys. D, 15, 1753
- Croft, R.A.C., Hu, W., Dave, R. 1999, PRL, 83, 1092
- de Bernardis, P. et al. 2000, Nature, 404, 955
- Dodelson, S., Kaplinghat, M., Stewart, E., 2000, PRL, 85, 5276
- Dunkley, J., Bucher, M., Ferreira, P. G., Moodley, K., Skordis K. 2005, Mon. Not. R. Astron. Soc., 356, 925
- Dunkley, J., Komatsu, E., Nolte, M. R., Spergel, D. N., et al. 2009, ApJ Suppl., 180, 306
- Eisenstein, D. et al. 2005, ApJ, 633, 560
- Eke, V.R., Cole, S., Frenk, C.S., Petrick, H.J. 1998, MNRAS, 298, 1145
- Feng, B., Li, M., Piao, Y.-S., Zhang, X. 2006, Phys. Lett. B, 634, 101
- Frieman, J., Hill, C., Stebbins, A., Waga, I. 1995, PRL, 75, 2077
- Gelman, A., Rubin, D. 1992, Statistical Science, 7, 457
- Hastings, W.K. 1970, Biometrika, 57, 97
- Hicken, M., et al. 2009, ApJ, 700, 331-357

- Hicken, M., Wood-Vasey, W. M., Blondin, S., Challis, P., Jha, S., Kelly, P. L., Rest, A., Kirshner, R. P., 2009, *ApJ*, 700, 1097
- Jain, D., Dev, A., and Alcaniz, J.S. 2007, *PLB*, 656, 15
- Jeffreys, H., 1961, *Theory of Probability*, Oxford University Press, Oxford, 3rd ed.F
- Jiménez, R., Loeb, A., 2002, *ApJ*, 573, 37
- Jiménez, R., Verde, L., Treu, T., Stern, D., 2003, *ApJ*, 593, 622
- Jiménez, R., MacDonald, J., Dunlop, J.S., Padoan, P., Peacock, J.A., 2004, *MNRAS*, 349, 240
- Kurek, A., Hrycyna, O., Szydlowski, M., 2008, *arXiv:0805.4005*
- Kodama, Y., Yonetoku, D., Murakami, T., Tanabe, S., Tsutsui, R., Nakamura, T., 2008, *MNRAS*, 391, L1
- Kowalski, M., Rubin, D., Aldering, G. et al., 2008, *ApJ*, 686, 749
- Le Fèvre, O., et al., 2005, *A&A*, 439, 845
- Leng, C., preprint (*arXiv:0711.1918*)
- Liddle, A. R., 2004, *MNRAS*, 351, L49
- Liddle, A. R., Mukherjee, P., Parkinson, D., 2006, *A&G*, 47, 4.30
- Liddle, A. R., 2007, *MNRAS*, 377, L74
- Linder, E. V., 2003, *PRL*, 90, 091301
- Linder, E. V., Dragan, H., 2005, *PRD*, 72, 043509
- Linder, E. V., 2006, *Astroparticle Physics*, 25, 167
- Liu, J. and Li, H. and Xia, J. Q. and Zhang, X., 2009, *JCAP*, 0907, 017
- McDonald, P. et al., 2005, *ApJ*, 635, 761
- MacKay, D. J. C., 2003, *Information Theory, Inference, and Learning Algorithms*, Cambridge University Press
- Metropolis, N., et al., 1953, *JCP*, 21, 1087
- Neal, R.M., 25 September 1993, *Technical Report CRG-TR-93-1*, Department of Computer Science, University of Toronto
- Padmanabhan, T. 2003, *PR*, 380, 235
- Peebles, P.J.E., Ratra, B. 2003, *RMP*, 75, 559
- Pope, A.C. et al. 2005, *ApJ*, 607, 655
- Refregier, A. 2003, *ARA&A*, 41, 645
- Riess, A.G. et al., 2004, *ApJ*, 607, 665
- Riess, Adam G. et al., 2007, *ApJ*, 609, 98
- Riess, Adam G. et al., 2009, *ApJ*, 699, 539
- Sáez-Gómez, D., 2009, *G&C*, 15, 134
- Sahni, V., Wnag, L., 2000, *PRD*, 62, 103517
- Sánchez, A.G. et al., 2006, *MNRAS*, 366, 189
- Schwarz, G., 1978, *Annals of Statistics*, 5, 461
- Shafieloo, A. et al., 2009, *PRD*, 80,101301
- Simon, J., Verde, L., Jiménez, R., 2005, *PRD*, 71, 123001
- Seljak, U. et al., 2005, *PRD*, 71, 103515
- Spergel, D.N. et al., 2003, *ApJS*, 148, 175
- Spiegelhalter D. J., Best N. G., Carlin B. P., van der Linde A., 2002, *J. R. Statist. Soc. B*, 64, 583
- Stern, D., 2000, preprint (*astro-ph/0012146*)
- Stern, D., Jiménez, R., Verde, L., Kamionkowski, M., Stanford, S.A., 2010, *JCAP*, 1002, 008
- Stern, D., Jiménez, R., Verde, L., Stanford, S.A., Kamionkowski, M., 2009, preprint (*arXiv:0907.3152*)
- Sullivan, S., Sarkar, D., Joudaki, S., Amblard, A., Holz, D.E. and Cooray, A. 2008, *PRL*, 100, 241302
- Takeuchi, T.T., *Ap&SS*, 271, 213
- Tegmark, M. et al. 2004, *PRD*, 69, 103501
- Viana, P.T.P., Nichol, R.C., Liddle, A.R., 2002, *ApJ*, 569, 75
- van Waerbeke, L. et al., 2001, *A&A*, 374, 757
- Yonetoku, D., Murakami, T., Nakamura, T., Yamazaki, R., Inoue, A.K., Ioka, K., 2004, *ApJ*, 609, 935
- Xia, J. Q. and Feng, B. and Zhang, X., 2005, *MPLA* 20, 2409
- Xia, J. Q., and Li, H. and Zhao, G. B. and Zhang, X., 2008, *IJMPD*, 17, 2025
- Xia, J. Q. and Zhao, G. B. and Li, H. and Feng, B. and Zhang, X., 2006, *PRD*, 74, 083521